HHS Public Access

Author manuscript

Hepatology. Author manuscript; available in PMC 2017 September 01.

Published in final edited form as:

Hepatology. 2016 September ; 64(3): 894–907. doi:10.1002/hep.28603.

Glutathione Antioxidant Pathway Activity and Reserve Determine Toxicity and Specificity of the Biliary Toxin Biliatresone in Zebrafish

Xiao Zhao[1], **Kristin Lorent**[1], **Benjamin Wilkins**[2], **Dylan M. Marchione**[3], **Kevin Gillespie**[3], **Orith Waisbourd-Zinman**[4], **Juhoon So**[5], **Kyung Ah Koo**[6], **Donghun Shin**[5], **John R. Porter**[6], **Rebecca G. Wells**[1], **Ian Blair**[3], and **Michael Pack**[1,7]

[1] Division of Gastroenterology, Department of Medicine, Perelman School of Medicine, University of Pennsylvania, Philadelphia, PA 19104, USA.

[2] Department of Pathology and Laboratory Medicine, Children's Hospital of Philadelphia, Philadelphia, PA 19104, USA.

[3] Department of Systems Pharmacology and Translational Therapeutics, Perelman School of Medicine, University of Pennsylvania, Philadelphia, PA 19104, USA.

[4] Division of Gastroenterology, Hepatology and Nutrition, Children's Hospital of Philadelphia, Philadelphia, PA 19104, USA.

[5] Department of Developmental Biology, McGowan Institute for Regenerative Medicine, University of Pittsburgh, Pittsburgh, PA 15260, USA.

[6] Department of Biological Sciences, University of the Sciences, Philadelphia, PA 19104, USA.

[7] Cell and Developmental Biology, Perelman School of Medicine, University of Pennsylvania, Philadelphia, PA 19104, USA.

Abstract

Biliatresone is an electrophilic isoflavone isolated from *Dysphania* species plants that has been causatively linked to naturally occurring outbreaks of a biliary atresia (BA)-like disease in livestock. Biliatresone has selective toxicity for extrahepatic cholangiocytes (EHC) in zebrafish larvae. To better understand its mechanism of toxicity, we performed transcriptional profiling of liver cells isolated from zebrafish larvae at the earliest stage of biliatresone-mediated biliary injury, with subsequent comparison of biliary and hepatocyte gene expression profiles. Transcripts encoded by genes involved in redox stress response, particularly those involved in glutathione (GSH) metabolism, were among the most prominently upregulated in both cholangiocytes and hepatocytes of biliatresone-treated larvae. Consistent with these findings, hepatic GSH was depleted at the onset of biliary injury, and *in situ* mapping of the hepatic GSH redox potential using a redox-sensitive GFP (roGFP) biosensor showed that it was significantly more oxidized in EHC both before and after treatment with biliatresone. Pharmacological and genetic manipulation

Corresponding author: Michael Pack, MD, Gastroenterology Division, Department of Medicine, University of Pennsylvania School of Medicine, Rm 1113 BRB 2/3, 421 Curie Blvd., Philadelphia, PA 19104, Tel 215-573-4145, Fax 215-898-9871, mpack@mail.med.upenn.edu.

of GSH redox homeostasis confirmed the importance of GSH in modulating biliatresone-induced injury as GSH depletion sensitized both EHC and the otherwise resistant intrahepatic cholangiocytes (IHC) to the toxin, whereas replenishing GSH level *via N*-acetylcysteine administration or activation of nuclear factor, erythroid 2-like 2 (Nrf2), a transcriptional regulator of GSH synthesis, inhibited EHC injury. Conclusion: These findings strongly support redox stress as a critical contributing factor in biliatresone-induced cholangiocyte injury, and suggest variations in intrinsic stress responses underlie the susceptibility profile. Insufficient antioxidant capacity of EHC may be critical to the early pathogenesis of human BA.

Keywords

Biliary atresia; cholangiocytes; Nrf2; redox stress

Biliary atresia (BA) is a neonatal cholangiopathy that is the most common cause of infantile cholestasis and the most common indication for liver transplantation in the pediatric population (1). It is characterized by progressive fibro-obliteration of the extrahepatic bile ducts (EHD), and occurs in approximately one out of 5000-15,000 births (2). Although adequate biliary drainage can be restored in the majority of patients *via* Kasai portoenterostomy, nearly all patients develop intrahepatic biliary injury that progresses to biliary cirrhosis. Half of the afflicted children require liver transplant by age 2, and the majority before reaching adulthood (3). Indeed, BA is a major cause of liver-related morbidity and mortality in the pediatric population (4).

It is increasingly evident that BA is a complex disease in which the interplay between environmental agents and genetic factors together confer susceptibility to biliary injury (5, 6). While such environmental etiologies remain obscure in humans, recurrent epidemics of naturally occurring BA-like disease have been reported in newborn Australian livestock (7). All of the outbreaks occurred during drought conditions and were linked to maternal ingestion of atypical pasturage with an abundance of plants in the genus *Dysphania*. By use of an *in vivo* zebrafish biliary secretion assay, we recently isolated a novel electrophilic isoflavone, biliatresone, from *Dysphania* extracts that has selective extrahepatic biliary toxicity (8, 9). The phenotype induced in this new toxin-mediated BA model is conserved between zebrafish and mammals, and recapitulates the cardinal features of human BA (8). The discovery of biliatresone provides a novel opportunity to study mechanisms underlying the pathogenesis of BA and potentially other cholangiopathies.

The selective toxicity of biliatresone towards extrahepatic cholangiocytes (EHC) is one of the most striking features of the *Dysphania* BA syndrome. We previously showed that this can be explained in part by its biliary secretion (8), and presumably, enterohepatic metabolism, which is known to occur with isoflavones present in soy and other consumable plants (10). It remains unclear, however, why hepatocytes and intrahepatic cholangiocytes (IHC), which synthesize and transport bile, respectively, are resistant to biliatresone *in vivo*. One clue comes from *in vitro* studies that reveal biliatresone as a strong oxidant capable of forming adducts with glutathione (GSH), histamine, and amino acids at its alpha-methylene moiety, which functions as a Michael acceptor (9, 11). The reactivity of biliatresone towards

these bioactive molecules suggests that extrahepatic biliary injury in the *Dysphania* BA syndrome may be caused by redox and/or proteomic stresses within EHC, and that resistant cells (hepatocytes and IHC) are able to mitigate these stresses.

Eukaryotic cells have evolved complex mechanisms to prevent deleterious oxidative modifications of cellular macromolecules (12). The tripeptide GSH plays a crucial role in cytoprotective antioxidative responses, and acts as a nucleophilic scavenger of xenobiotics, such as biliatresone. Because of its essential role in multiple aspects of cellular physiology (13), GSH synthesis is tightly regulated (14). The rate-limiting step is generation of a *gamma* peptide linkage between cysteine and glutamate by *gamma*-glutamyl cysteine ligase (Gcl). Regulation of the genes encoding the Gcl subunits, *Gclc* and *Gclm*, is largely mediated by nuclear factor, erythroid 2 (Nrf2), a transcription factor that is considered the master regulator of the antioxidant response (15). Under physiological conditions, most Nrf2 is degraded through the ubiquitinproteasome pathway in a kelch-like ECH-associated protein 1 (Keap1)-dependent manner. However, electrophiles and reactive oxygen species can bind to and alter the conformation of Keap1 by modifying its thiol residues, leading to translocation of Nrf2 to the nucleus where it heterodimerizes with small Maf proteins. Nrf2-Maf heterodimers then bind the antioxidant response element (ARE) enhancer present in the promoter of many antioxidant genes (16, 17).

Given the importance of Nrf2-mediated responses in mitigating electrophilic stress, we hypothesized that differential activity of this pathway may be a determining factor in the cellular susceptibility to biliatresone. Supporting this idea, Nrf2 has previously been shown to play an important role in bile acid homeostasis, and its deletion results in multiple adaptive changes in bile acid synthesis and metabolism, resembling a cholestatic phenotype (18). Nrf2 knockout mice are also sensitized to injury induced by lithocholic acid, a highly toxic secondary bile acid (19). Most recently, levels of NRF2 were also shown to be elevated in cholangiocytes of patients with cholestatic diseases, including BA, likely reflecting ongoing oxidative stress due to reduced bile flow (20).

In this study, we present extensive experimental evidence in support of the critical role of GSH and Nrf2-mediated redox signaling in the early pathogenesis of toxin-induced BA in the zebrafish model. Our findings confirm that the electrophilic properties of biliatresone are responsible for its toxicity, and its specificity is driven at least in part by differential basal and inducible redox responses among different liver cell types.

Materials and Methods

Zebrafish Lines

The wild-type strains (TL, AB), transgenic strains (*Tg(krt18:TRAP)*; *Tg(fabp10a:TRAP)*; *Tg(ef1a:Grx-roGFP; Tg(Tp1:mCherry)*; *Tg(Tp1:EGFP)*) and the *nrf2* mutant strain (*nfe2l2a*^{fh318} allele) were used for the present studies. The *nrf2* mutant fish were genotyped using the KASP genotyping assays (KBioscience). All zebrafish were raised in the University of Pennsylvania School of Medicine zebrafish facility in accordance with protocols approved by the University of Pennsylvania Institutional Animal Care and Use Committee.

Zebrafish bioassay and analyses

Zebrafish larvae reared in 24-well plates were exposed to lyophilized biliatresone resuspended in anhydrous DMSO for 4 to 24 hours (hr) (final concentration, 0.5% DMSO in embryo medium), depending on the experiments. The concentrations of biliatresone varied with the experimental conditions, and ranged from 0.25 to 0.50 μg/ml. All assays were repeated three times with at least 30 treated larvae and an equal number of control larvae.

For the sensitization or rescue experiments, larvae were placed in 24-well plates with embryo medium containing sulforaphane (SFN) (Sigma), *N*-acetylcysteine (NAC) (Sigma), or buthionine sulfoximine (BSO) (Sigma). The E3 medium containing each compound was changed daily. After chemical treatments, larvae were fixed in 4% paraformaldehyde and immunostained with mouse monoclonal antibody Annexin A4 (ABCAM), rabbit monoclonal anti-GFP (ABCAM), or processed for confocal microscopy and/or histology as previously described (8). Increased gain was applied to samples if necessary to visualize hypoplastic intrahepatic ducts.

RNA-seq

Fifty livers and their associated extrahepatic biliary ducts, were dissected from DMSO-treated and biliatresone-treated (0.5 μg/ml, 4 hr) wild-type larvae and 1 μg of total RNA was isolated using the standard Qiagen protocol (Rneasy Mini kit). The experiment was done with two sets of biological replicates. The extracted RNA was submitted to the CHOP Genomics Core for library construction with the Truseq Stranded RiboZero kit (Illumina) followed by sequencing on the HiSeq2000 paired-end 100 bp platform. RNA-seq reads were mapped to the zebrafish reference genome and RefSeq transcriptome (zv9) using the STAR software. Counting of reads per gene was performed using Htseq. Differential expression of transcript reads between biliatresone-treated larval livers and DMSO-treated controls was analyzed with the DeSeq package. These data are available *via* the Gene Expression Omnibus (GEO) at accession number GSE76780.

Nanostring nCounter assay and data analysis

Actively translating mRNA was extracted from larval hepatocytes and cholangiocytes (*Tg(fabp10a:TRAP)*; (*Tg(krt18:TRAP)*) using the translating ribosomal affinity purification (TRAP) methodology as previously described (21). Gene expression analysis was performed with the nCounter system (NanoString Technologies) as previously described (22). The input RNA was 100 ng per sample. The nCounter system uses molecular barcodes for direct digital detection of individual target mRNA molecules. The raw data were first normalized to the positive controls provided by the manufacturer, which accounted for variations in hybridization and purification efficiency, and then to three housekeeping genes (*bactin2*, *ef1a*, *rpl19*). The experiment was done in three biological replicates and differential gene expression was calculated relative to DMSO-treated controls.

GSH derivatization and Liquid Chromatography-Mass Spectrometry (LC/MS)

The procedures were modified from a previously published protocol (23). Five larval livers (including the extrahepatic biliary system) were used per sample. Additional details are described in the supplementary section.

roGFP redox mapping

Double transgenic (*Tg(ef1a:Grx-roGFP*; *tp1:mCherry*)) larvae were used for the redox mapping of hepatocytes, IHC and EHC. *Tg(ef1a:Grx-roGFP)* is a redox biosensor line previously generated in our laboratory (24). Conservation of the biosensor redox state was achieved with the thiol-alkylating agent *N*-Ethylmaleimide (NEM) and the protocol was adapted from a previous study of deep tissue fluorescence redox imaging in adult *Drosophila* (25). Additional details are described in the supplementary section.

Statistical analyses

Data represent at least three independent experiments reported as means +/− standard error of the mean. Student's *t* test was used for comparison between two groups. Data from three or more groups were analyzed by one-way analysis of variance (ANOVA) with Tukey's multiple comparisons test. $p < 0.05$ was considered to be significant.

Results

Biliatresone leads to the activation of multiple evolutionarily conserved stress pathways, including GSH redox cycling and the Nrf2-Keap1 regulatory network

In order to elucidate the molecular mechanisms underlying biliatresone-induced injury, we transcriptionally profiled liver RNA isolated from biliatresone (0.5 μg/ml)-treated larval zebrafish and their DMSO-treated control siblings *via* RNA-seq. Livers and their associated extrahepatic biliary ducts were dissected 4 hr after biliatresone incubation, when the extrahepatic ducts exhibited only signs of minimal injury. Multiple evolutionarily conserved stress signaling pathways were induced after biliatresone exposure, including those involved in the cellular redox response, heat shock response, and unfolded protein response (UPR)/ endoplasma reticulum (ER) stress (Table S1; GEO dataset GSE76780). We noted significant upregulation of genes involved in phase II detoxification, specifically, those encoding for enzymes required for GSH biosynthesis (*gclc*, *gclm*) and metabolism (*glutathione S-transferase (gsto1*, *gstp1*)). Induction of the phase II detoxification pathway is largely controlled by activation of Nrf2-mediated gene transcription (26). Supporting this, we also observed significant upregulation of other Nrf2 targets including *keap1a, keap1b,* and *sequestosome-1 (sqstm1)*.

Cell-type specific transcriptional profiling experiments indicated that both cholangiocytes and hepatocytes activate cytoprotective pathways in the initial cellular defense against biliatresone. Profiling of polysomal mRNA isolated from larval biliary cells (EHC & IHC) and hepatocytes via TRAP (18) revealed induction of antioxidant genes in both cell types 4 hr after biliatresone exposure. Some genes were induced more prominently in biliary cells than hepatocytes (*gclm*,*gsto1*, *keap1a)* (Fig. 1A). These data suggest that biliatresone induces redox stress, which in turn activates the Nrf2-Keap1 pathway, leading to compensatory stimulation of GSH synthesis and conjugation. They are also consistent with the *in vitro* electrophilic properties of biliatresone.

Biliatresone leads to hepatic GSH depletion

Based on our RNA-seq data, we hypothesized that biliatresone would deplete GSH in the larval zebrafish liver, either through secretion of the biliatresone-GSH conjugate into bile, and/or oxidation of GSH to GSSG. We tested these possibilities by measuring GSH content directly through mass spectrometry in livers (including extrahepatic bile ducts) dissected from biliatresone-treated and their sibling control larvae (n=5 larvae in each pool). These experiments showed that biliatresone exposure indeed led to a dose dependent decrease in GSH level (Fig. 1B). Compared to control larvae, GSH level was reduced by 53.6% after 4 hr of incubation with the standard dose of biliatresone (0.5 μg/ml). This decrease persisted after 12 hr of treatment; interestingly, the GSH pool was replenished by 24 hr, suggesting that the GSH biosynthetic and recycling machinery is able to compensate for the loss over time. We observed a less pronounced and non-significant reduction of GSH content with the lower non-toxic dose of biliatresone (0.25 μg/ml) after both 4 hr and 12 hr of exposure (Fig. 1B). Measurement of GSH levels in the matched intestine and remnant larval integument after 12 hr of biliatresone treatment at 0.5 μg/ml showed no significant change compared to control larvae (Fig. S1).

Hepatocytes and EHC exhibit endogenous differences in both basal redox state and response to biliatresone

Although biliatresone treatment significantly reduced hepatic GSH levels, our analyses could not tell us whether it had comparable effects in resistant (hepatocytes, IHC) *versus* sensitive (EHC) cells. Furthermore, it was unclear whether the GSH reduction was caused by differences in the basal redox status among different liver cell types, variation in their response to electrophilic stress, or a combination of these factors. To address these questions, we measured GSH redox state at baseline and after biliatresone exposure in hepatocytes, IHC and EHC with a genetically-encoded redox-sensitive green fluorescent protein (roGFP2). roGFP2 contains an engineered dithiol/disulfide switch that provides a redox-sensitive ratiometric readout of emission at two excitation wavelengths (405 nm, 488 nm). When fused with glutaredoxin-1 (Grx1), it is a highly sensitive and specific probe that can be used to detect rapid minute changes in the intracellular GSH redox potential. A high fluorescence ratio indicates an oxidized sensor, whereas a low redox fluorescence ratio signifies a reduced state (25). We used Grx1-roGFP2 to first map the baseline cytosolic GSH redox state of larval zebrafish hepatic cells. In order to avoid perturbing the endogenous redox state, we performed our analyses with tissues prepared in the presence of NEM, a highly effective thiol-alkylating agent that prevents roGFP2 oxidation during the dissection and fixation processes (25). Interestingly, we found significant heterogeneity in the basal redox state between cells within the liver parenchyma and the extrahepatic biliary tree (gallbladder). While hepatocytes and IHC were consistently found in a highly reduced state, gallbladder epithelium clearly had a more oxidized GSH pool (Fig. 1C, D). We repeated these measurements after biliatresone exposure. Although all three cell types were oxidized by biliatresone, the change was markedly more pronounced in the gallbladder epithelium (Fig. 1C, D). These observations indicate that there are endogenous variations in redox homeostasis among different liver cell types, and EHC may be particularly susceptible to electrophilic injury due to a low GSH reserve.

Administration of the GSH precursor NAC attenuates biliatresone toxicity

Since biliatresone led to GSH depletion, we sought to determine whether the toxicity was attenuated by co-treatment of larvae with NAC, a well-described GSH precursor that is used to treat acetaminophen toxicity (27). We compared biliary morphology in larvae treated with either biliatresone or biliatresone and NAC *via* confocal microscopy using a monoclonal antibody directed against Annexin A4, which stains bile duct cells (28). Changes in gallbladder morphology detected using this approach quantitatively correlate with biliary secretion (8). These experiments showed that NAC treatment did indeed block biliatresone toxicity. As opposed to the dramatic extrahepatic biliary injury observed in 89.7% of larvae exposed to biliatresone (0.5 μg/ml, 16 hr), co-administration of NAC (20 μM) inhibited biliary toxicity in 73.8% of larvae examined. A lower dose of NAC (10 μM) was not effective (Fig. 2A, B). To ensure that NAC was indeed contributing to the GSH pool, we measured GSH levels in larval livers by mass spectrometry after 16 hr of treatment. In contrast to the significant decline in the GSH pool observed in larvae treated with biliatresone alone, GSH level was not significantly altered after co-treatment with NAC (20 μM). Interestingly, NAC treatment alone did not lead to an increase in hepatic GSH level (Fig. 2C).

Inhibition of GSH synthesis sensitizes EHC and the normally resistant IHC to biliatresone

The observation that NAC protects larvae from biliatresone-mediated biliary injury suggests that maintaining GSH homeostasis may play a crucial role in the initial defense against this toxin. We next sought to determine whether inhibition of GSH synthesis would sensitize larvae to a minimally toxic dose of biliatresone. We pretreated larvae starting at 3 day post-fertilization (dpf) with BSO (1 mM), a specific inhibitor of *de novo* GSH synthesis (29), for 48 hr followed by the addition of low-dose biliatresone (0.25 μg/ml) for 12 hr (Fig. 3A). As expected, 66.3% of larvae treated with low-dose biliatresone exhibited no apparent biliary toxicity, while the remainder had only minor changes in EHD morphology. In contrast, with BSO pre-treatment, low-dose biliatresone exposure led to extensive EHD injury as evidenced by destruction of the gallbladder in 83.3% of larvae (Fig. 3B, C). Furthermore, the usually resistant intrahepatic bile ducts (IHD) were injured in 72.2% of larvae with Annexin A4 immunostains highlighting a paucity of ductular projections compared to controls (Fig. 3B, C). The sensitization of IHD to biliatresone caused by reduction of GSH reserve was confirmed in a separate transgenic line that expresses EGFP in IHC (*Tg*(*Tp1:EGFP*)) (Fig. S2). Interestingly, if we co-administered BSO with low-dose biliatresone for 12 hr in larvae without BSO pre-treatment, we observed destruction of EHC but the intrahepatic system appeared unaffected (Fig. S3). This suggests that intrahepatic biliary cells, as opposed to EHC, have sufficient GSH reserve at baseline to combat biliatresone, and prior depletion of this reserve is necessary for sensitization.

To examine the degree of GSH reduction by BSO, we again measured the GSH level in larval liver *via* mass spectrometry. BSO treatment alone resulted in 75.4% decrease in GSH content compared to control larvae. Interestingly, this significant decline did not affect larval viability or lead to hepatocyte or biliary injury (Fig. 3B-D). Addition of low-dose biliatresone (0.25 μg/ml) after BSO pre-treatment led to further depletion of GSH, whereas this dose of biliatresone alone did not significantly affect the overall hepatic GSH level (Fig.

3D). Collectively, these data suggest that although GSH depletion by itself is not deleterious, it does crucially affect the ability of cholangiocytes (EHC and IHC) to combat electrophilic stress.

nrf2 mutant zebrafish larvae are sensitized to biliatresone and have reduced hepatic GSH reserve

Since Nrf2 is considered the master regulator of the cellular antioxidant responses and appears to be activated during biliatresone exposure, we asked whether genetic disruption of Nrf2 would sensitize larvae to biliatresone. The *nfe2l2a*^{fh318} allele encodes a missense mutation (R485L) in the Nrf2a protein that has been shown previously to reduce transcriptional activation of antioxidant genes (29). Homozygous *nfe2l2a* mutants (hereafter *nrf2* mutants), which develop normally under unstressed conditions and are fertile, tolerated low-dose biliatresone (0.25 μg/ml, 12 hr) with no increase in mortality. The treatment, however, induced typical EHD injury in 67.8% of mutant larvae by 12 hr (Fig. 4A-B', D). Furthermore, by 24 hr, the usually resistant IHD appeared hypoplastic with prominent cell bodies and shorter ductular projections in 80.0% of livers (Fig. 4B", D). These abnormalities became even more apparent in mutant larvae that were treated with BSO for 48 hr to deplete GSH prior to low-dose biliatresone (0.25 μg/ml) incubation. Notably, we observed these defects after only 12 hr of biliatresone exposure, and 100% mortality was observed at 24 hr (Fig. 4C-D). Interestingly, although there was no histological evidence of hepatocyte injury in the biliatresone-treated *nrf2* mutants (Fig. S4), ultrastructural analyses showed dilation and distortion of the ER, a finding suggestive of ER stress (Fig. S5).

As Nrf2 stimulates GSH synthesis, we determined hepatic GSH levels in *nrf2* mutants and wild-type controls. Baseline hepatic GSH was reduced by 45.0% in mutant larvae compared to their wild-type siblings (Fig. 5A). Furthermore, low-dose biliatresone (0.25 μg/ml) treatment led to a greater reduction in hepatic GSH than that achieved with the higher dose (0.50 μg/ml) in sibling wild-type larvae. We also examined hepatic expression of phase II metabolism genes and other Nrf2 targets in *nrf2* mutant larvae and sibling wild-type controls following 4 hr of biliatresone exposure (0.50 μg/ml). Although mRNA expression levels of genes involved in GSH synthesis and utilization were increased in *nrf2* mutants, indicating compensation by other *nrf2* family genes or Nrf2-independent pathways, the increase was significantly less than in wild-type larvae (Fig. 5B). Altogether, these results suggest that both constitutive and inducible hepatic GSH contribute to neutralizing redox stress incurred during biliatresone exposure.

The Nrf2 activator SFN delays the onset of biliatresone-induced biliary injury

SFN, an isothiocyanate originally isolated from broccoli, is a well-known Nrf2 activator in mammals and zebrafish (30, 31). We hypothesized that SFN would attenuate biliatresone-induced biliary injury through Nrf2 activation. To test this possibility, we pretreated wild-type larvae with SFN (20 μM) for 12 hr prior to treatment with biliatresone, and then continued treatment with SFN in the presence of biliatresone (0.5 μg/ml) for an additional 16 hr (Fig. 6A). SFN inhibited EHD injury in 73.9% of larvae pre-treated with SFN (Fig. 6B, C). Interestingly, the toxicity was not altered by SFN co-treatment in the absence of pre-treatment (Fig. S6), indicating that pre-activation of Nrf2 is required to inhibit the toxicity.

SFN also did not attenuate biliatresone toxicity in *nrf2* mutants (Fig. 6B, C), confirming that in zebrafish SFN exerts its protective effect against biliatresone *via* activation of Nrf2. We examined the effect of SFN on hepatic GSH level by mass spectrometry. Just as with NAC, SFN treatment on its own did not significantly affect GSH concentration; however, it did prevent GSH depletion in biliatresone-treated larvae (Fig. 6D).

Discussion

Despite extensive efforts to understand its etiology and pathogenesis, BA remains an enigmatic disease (32, 33). Perinatal damage from exposure to a virus or toxin has been long suspected based on time-space clustering of cases. Indeed, the most widely studied animal model of BA, which recapitulates many features of the human disease, including fibrotic obstruction of the common bile duct and reactive changes within the intrahepatic biliary system, utilizes infection of newborn Balb/C mice with *Rhesus* rotavirus (RRV) (34). Although rotavirus infection has not been implicated conclusively in human BA (35), the RRV model has provided the foundation for our understanding of the essential role of immunity and inflammation in BA pathogenesis (34, 36, 37). The *Dysphania* BA syndrome, initially described in newborn Australian livestock, then recapitulated in zebrafish by administration of biliatresone, provides the first *in vivo* evidence supporting a causative role of an environmental toxin in the pathogenesis of BA (7, 8). As we are interested in the mechanisms underlying the selective toxicity of biliatresone toward EHC, the focus of this study was to define cellular responses to biliatresone in sensitive and resistant liver cell types.

Our principal findings, derived from molecular and biochemical studies, are the following: First, exposure to biliatresone leads to activation of evolutionarily conserved stress pathways in larval liver, including the Nrf2-Keap1 redox signaling cascade. Second, biliatresone causes transient and selective depletion of hepatic GSH. Third, EHC exhibit a more oxidized GSH redox state at baseline and after biliatresone exposure compared to hepatocytes and IHC. Fourth, depletion of GSH sensitizes both EHC and the otherwise resistant IHC to the toxic effect of biliatresone. Fifth, replenishing GSH level *via* NAC administration or Nrf2 activation markedly attenuates biliatresone-induced biliary toxicity. Collectively, these findings indicate that biliatresone activates hepatic redox stress response pathways, and its selective toxicity may be explained by the gradient of GSH reserve that exists among the different liver cell types. These data provide novel insights into the molecular mechanisms underlying early cholangiocyte injury in BA pathogenesis, and may offer critical information about the role of GSH redox balance and the antioxidant response in the pathobiology of other cholangiopathies. In BA, we speculate that inadvertent maternal exposure to oxidants like biliatresone may alter the metabolism of otherwise non-toxic environmental electrophiles, leading to the lowering of fetal GSH reserve and predisposition to EHC injury.

The liver has long been recognized as a reservoir for GSH. In mammals, nearly all plasma GSH is derived from the sinusoidal efflux of GSH synthesized by hepatocytes, which are uniquely suited for large scale GSH biosynthesis and transport (14). In addition to their expression of distinct membrane transporters that facilitate GSH entry into sinusoidal blood and bile, hepatocytes are the only cells that are capable of generating cysteine from

methionine *via* the transsulfuration pathway (14). This additional source of cysteine, beyond what is normally available from diet and protein catabolism, is important because cysteine is the rate-limiting substrate for *de novo* GSH synthesis (14). Other cell types including cholangiocytes derive their cellular access to cysteine from extracellular metabolism of GSH by the enzyme γ-glutamyl transpeptidase (GGT) (14). Therefore, the ability of hepatocytes to synthesize a large amount of GSH is important not only for cellular redox balance but also for organismal cysteine balance, which has to be tightly regulated to avoid cysteine toxicity (38).

Hepatic GSH levels in zebrafish larvae have not been reported previously; however, our *in vivo* redox mapping studies indicate a large GSH pool relative to GSSG in hepatocytes. Interestingly, while the redox potential of IHC is comparable to hepatocytes, EHC clearly exhibit a significantly more oxidized state than either cell type, both at baseline and after biliatresone treatment. The reason for this heterogeneity in basal and inducible GSH redox status, which correlates with susceptibility to biliatresone, is not known. Potential explanations include variation in cysteine uptake and/or differences in the levels or activity of Nrf2 as well as GSH synthesizing enzymes. Cell-type specific differences in the activity of γ-glutamylcysteine ligase (GCL), which is the rate-limiting enzyme for GSH synthesis, have also been reported (39). Interestingly, hepatocytes and IHC develop from a common progenitor cell, the hepatoblast, whereas EHC are derived from the caudal part of the ventral foregut endoderm (40). It is conceivable that the different embryonic origins contribute to the variation in redox state.

Whether there is a comparable degree of heterogeneity in the redox status of mammalian hepatocytes, IHC, and EHC is not known. GSH levels in IHC were previously shown to be approximately one-third of those in hepatocytes in adult rats (41). However, this study utilized cells recovered *via* proteolytic digestion that conceivably could have altered the redox balance. We recently observed that the GSH concentration in extrahepatic biliary ducts dissected from neonatal mice was 50% lower than in the liver parenchyma (Wells R, unpublished); however, IHC were not distinguished from EHC. Similarities in zebrafish and mammalian GSH metabolism were detected in our study, including a conserved role for Nrf2 in basal and inducible GSH synthesis (42), tight regulation of redox homeostasis as evidenced by unchanged GSH levels in response to NAC and SFN, and Nrf2-independent upregulation of GSH synthesis (14).

In contrast to these similarities, we found differences in the response between mammalian and zebrafish cholangiocytes to GSH depletion. Notably, BSO treatment induced apoptosis in cultured mammalian IHC (43). It also led to lumen occlusion and loss of polarity in mouse cholangiocyte spheroids as well as to monolayer abnormalities and fibrosis in neonatal EHBD explants (Wells R, unpublished). However, GSH depletion by itself was well-tolerated by both IHC and EHC in zebrafish. We saw no evidence of biliary injury despite 75% reduction in total hepatic GSH, which likely reflects GSH levels in cholangiocytes given their dependence on hepatocytes for GSH synthesis. This suggests that altered redox balance, on its own, is insufficient to induce injury, and that an additional oxidizing stimulus, such as biliatresone, is required. While this discrepancy can potentially be explained by intrinsic differences in animal models, it is also possible that *in vivo*

cholangiocytes are able to mitigate stress induced by GSH depletion compared to cells in cultured or *ex vivo* conditions.

Regardless of the underlying causes, the work reported in this study clearly shows that heterogeneity in hepatic GSH redox balance plays a fundamental role in determining the cellular susceptibility profile to biliatresone. Further experiments will more clearly define how the cholangiocyte electrophilic stress response is affected by modulation of GSH metabolism. These include measurement of GSH flux in larval hepatocytes, IHC, and EHC so that the basal and inducible rates of GSH synthesis can be correlated with the redox mapping data, and exploring the cell-type specific roles of GSH-coupled antioxidant enzymes, such as GSH-transferases, GSH-peroxidases, GSH-reductases, and glutaredoxins. It will be useful to define the potential role of other Nrf2-regulated antioxidant responses, as well as Nrf2-independent pathways in combating biliatresone-induced electrophilic stress. These include non-GSH redox-coupled antioxidant systems (*e.g.* thioredoxin), phase I and phase II enzymes that can metabolize biliatresone, and membrane transporters that may mediate secretion and/or efflux of biliatresone or its conjugate. Differences in baseline activity and inducible activation of these intrinsic defense mechanisms may account for the resistance of hepatocytes to biliatresone, even in the absence of Nrf2.

In summary, our study shows that redox stress signaling is important for mediating the response of cholangiocytes to toxic injury, and that endogenous variation in GSH redox potential may play a significant role in determining susceptibility to injury caused by xenobiotics, such as biliatresone. In addition to providing novel insights into the pathogenesis of BA, the difference in redox state may help explain why EHC and IHC are often differentially affected in human biliary diseases. Ultimately, this may have important implications for developing new therapeutic strategies for these uncommon yet important liver diseases.

Supplementary Material

Refer to Web version on PubMed Central for supplementary material.

Acknowledgements

The authors are grateful to the Children's Hospital of Philadelphia (CHOP) and the Beijing Genomics Institute (BGI) for the next generation sequencing service, the Department of Biomedical and Health Informatics at CHOP for bioinformatics support, the Cell and Developmental Biology Microscopy core and the Electron Microscopy core at the University of Pennsylvania for imaging support. We are grateful to Aiste Balciunaite, Jie He, Manimegalai Muthumani, and Xi Xu for technical contributions.

Financial support:

This research was supported by NIH/NIDDK grants R01 DK092111 to M.P., R.G.W, and J.R.P., 5T32DK007066 and the Center for Molecular Studies in Digestive and Liver Diseases Pilot Grant (P30DK050306) to X.Z., and by the Fred and Suzanne Biesecker Pediatric Liver Center.

List of Abbreviations

BA	biliary atresia
EHC	extrahepatic cholangiocytes

GSH	glutathione
roGFP	redox-sensitive green fluorescent protein
Nrf2	nuclear factor, erythroid 2-like
IHC	intrahepatic cholangiocytes
EHD	extrahepatic bile ducts
gcl	gamma-glutamyl cysteine ligase
Keap1	kelch-like ECH-associated protein 1
ARE	antioxidant response element
SFN	sulforaphane
NAC	*N*-acetylcysteine
BSO	buthionine sulfoximine
TRAP	translating ribosomal affinity purification
ABD-F	7-fluorobenz-2-oxa-1,3-diazole-4-sulfonamide
LC/MS	liquid chromatography-mass spectrometry
NEM	N-Ethylmaleimide
SEM	standard error of the mean
UPR	unfolded protein response
ER stress	Endoplasmic reticulum stress
gst	glutathione S-transferase
sqstm1	sequestosome-1
Grx1	glutaredoxin-1
dpf	day post-fertilization
IHD	intrahepatic bile ducts

References

1. Hartley JL, Davenport M, Kelly DA. Biliary atresia. Lancet. 2009; 374:1704–1713. [PubMed: 19914515]
2. Haber BA, Russo P. Biliary atresia. Gastroenterol Clin North Am. 2003; 32:891–911. [PubMed: 14562580]
3. Schreiber RA, Barker CC, Roberts EA, Martin SR, Alvarez F, Smith L, Butzner JD, et al. Biliary atresia: the Canadian experience. J Pediatr. 2007; 151:659–665. 665, e651. [PubMed: 18035148]

4. Migliazza L, Lopez Santamaria M, Murcia J, Gamez M, Clavijo J, Camarena C, Hierro L, et al. Long-term survival expectancy after liver transplantation in children. J Pediatr Surg. 2000; 35:5–7. discussion 7-8. [PubMed: 10646764]
5. Garcia-Barcelo MM, Yeung MY, Miao XP, Tang CS, Cheng G, So MT, Ngan ES, et al. Genome-wide association study identifies a susceptibility locus for biliary atresia on 10q24.2. Hum Mol Genet. 2010; 19:2917–2925. [PubMed: 20460270]
6. Tsai EA, Grochowski CM, Loomes KM, Bessho K, Hakonarson H, Bezerra JA, Russo PA, et al. Replication of a GWAS signal in a Caucasian population implicates ADD3 in susceptibility to biliary atresia. Hum Genet. 2014; 133:235–243. [PubMed: 24104524]
7. Harper P, Plant JW, Unger DB. Congenital biliary atresia and jaundice in lambs and calves. Aust Vet J. 1990; 67:18–22. [PubMed: 2334368]
8. Lorent K, Gong W, Koo KA, Waisbourd-Zinman O, Karjoo S, Zhao X, Sealy I, et al. Identification of a plant isoflavonoid that causes biliary atresia. Sci Transl Med. 2015; 7:286ra267.
9. Koo KA, Lorent K, Gong W, Windsor P, Whittaker SJ, Pack M, Wells RG, et al. Biliatresone, a Reactive Natural Toxin from Dysphania glomulifera and D. littoralis: Discovery of the Toxic Moiety 1,2-Diaryl-2-Propenone. Chem Res Toxicol. 2015; 28:1519–1521. [PubMed: 26175131]
10. Larkin T, Price WE, Astheimer L. The key importance of soy isoflavone bioavailability to understanding health benefits. Crit Rev Food Sci Nutr. 2008; 48:538–552. [PubMed: 18568859]
11. Koo KW-Z O, Wells R, Pack M, Porter J. Reactivity of Biliatresone, a Natural Biliary Toxin, with Glutathione, Histamine and Amino Acids. Chem Res Toxicol. 2015 In Press.
12. Fulda S, Gorman AM, Hori O, Samali A. Cellular stress responses: cell survival and cell death. Int J Cell Biol. 2010; 2010:214074. [PubMed: 20182529]
13. Dickinson DA, Forman HJ. Glutathione in defense and signaling: lessons from a small thiol. Ann N Y Acad Sci. 2002; 973:488–504. [PubMed: 12485918]
14. Lu SC. Glutathione synthesis. Biochim Biophys Acta. 2013; 1830:3143–3153. [PubMed: 22995213]
15. Wild AC, Moinova HR, Mulcahy RT. Regulation of gamma-glutamylcysteine synthetase subunit gene expression by the transcription factor Nrf2. J Biol Chem. 1999; 274:33627–33636. [PubMed: 10559251]
16. Lee JM, Johnson JA. An important role of Nrf2-ARE pathway in the cellular defense mechanism. J Biochem Mol Biol. 2004; 37:139–143. [PubMed: 15469687]
17. Hayes JD, Dinkova-Kostova AT. The Nrf2 regulatory network provides an interface between redox and intermediary metabolism. Trends Biochem Sci. 2014; 39:199–218. [PubMed: 24647116]
18. Weerachayaphorn J, Mennone A, Soroka CJ, Harry K, Hagey LR, Kensler TW, Boyer JL. Nuclear factor-E2-related factor 2 is a major determinant of bile acid homeostasis in the liver and intestine. Am J Physiol Gastrointest Liver Physiol. 2012; 302:G925–936. [PubMed: 22345550]
19. Tan KP, Wood GA, Yang M, Ito S. Participation of nuclear factor (erythroid 2-related), factor 2 in ameliorating lithocholic acid-induced cholestatic liver injury in mice. Br J Pharmacol. 2010; 161:1111–1121. [PubMed: 20977460]
20. Weerachayaphorn J, Amaya MJ, Spirli C, Chansela P, Mitchell-Richards KA, Ananthanarayanan M, Nathanson MH. Nuclear Factor, Erythroid 2-Like 2 Regulates Expression of Type 3 Inositol 1,4,5-Trisphosphate Receptor and Calcium Signaling in Cholangiocytes. Gastroenterology. 2015; 149:211–222. e210. [PubMed: 25796361]
21. Wilkins BJ, Gong W, Pack M. A novel keratin18 promoter that drives reporter gene expression in the intrahepatic and extrahepatic biliary system allows isolation of cell-type specific transcripts from zebrafish liver. Gene Expr Patterns. 2014; 14:62–68. [PubMed: 24394404]
22. Laranjeiro R, Whitmore D. Transcription factors involved in retinogenesis are co-opted by the circadian clock following photoreceptor differentiation. Development. 2014; 141:2644–2656. [PubMed: 24924194]
23. Zhu P, Oe T, Blair IA. Determination of cellular redox status by stable isotope dilution liquid chromatography/mass spectrometry analysis of glutathione and glutathione disulfide. Rapid Commun Mass Spectrom. 2008; 22:432–440. [PubMed: 18215009]

24. Seiler C, Davuluri G, Abrams J, Byfield FJ, Janmey PA, Pack M. Smooth muscle tension induces invasive remodeling of the zebrafish intestine. PLoS Biol. 2012; 10:e1001386. [PubMed: 22973180]
25. Albrecht SC, Barata AG, Grosshans J, Teleman AA, Dick TP. In vivo mapping of hydrogen peroxide and oxidized glutathione reveals chemical and regional specificity of redox homeostasis. Cell Metab. 2011; 14:819–829. [PubMed: 22100409]
26. Itoh K, Chiba T, Takahashi S, Ishii T, Igarashi K, Katoh Y, Oyake T, et al. An Nrf2/small Maf heterodimer mediates the induction of phase II detoxifying enzyme genes through antioxidant response elements. Biochem Biophys Res Commun. 1997; 236:313–322. [PubMed: 9240432]
27. Lauterburg BH, Corcoran GB, Mitchell JR. Mechanism of action of N-acetylcysteine in the protection against the hepatotoxicity of acetaminophen in rats in vivo. J Clin Invest. 1983; 71:980–991. [PubMed: 6833497]
28. Zhang D, Golubkov VS, Han W, Correa RG, Zhou Y, Lee S, Strongin AY, et al. Identification of Annexin A4 as a hepatopancreas factor involved in liver cell survival. Dev Biol. 2014; 395:96–110. [PubMed: 25176043]
29. Mukaigasa K, Nguyen LT, Li L, Nakajima H, Yamamoto M, Kobayashi M. Genetic evidence of an evolutionarily conserved role for Nrf2 in the protection against oxidative stress. Mol Cell Biol. 2012; 32:4455–4461. [PubMed: 22949501]
30. Keum YS. Regulation of the Keap1/Nrf2 system by chemopreventive sulforaphane: implications of posttranslational modifications. Ann N Y Acad Sci. 2011; 1229:184–189. [PubMed: 21793854]
31. Kobayashi M, Li L, Iwamoto N, Nakajima-Takagi Y, Kaneko H, Nakayama Y, Eguchi M, et al. The antioxidant defense system Keap1-Nrf2 comprises a multiple sensing mechanism for responding to a wide range of chemical compounds. Mol Cell Biol. 2009; 29:493–502. [PubMed: 19001094]
32. Bezerra JA. Potential etiologies of biliary atresia. Pediatr Transplant. 2005; 9:646–651. [PubMed: 16176425]
33. Mack CL, Feldman AG, Sokol RJ. Clues to the etiology of bile duct injury in biliary atresia. Semin Liver Dis. 2012; 32:307–316. [PubMed: 23397531]
34. Mack CL. The pathogenesis of biliary atresia: evidence for a virus-induced autoimmune disease. Semin Liver Dis. 2007; 27:233–242. [PubMed: 17682970]
35. Saito T, Shinozaki K, Matsunaga T, Ogawa T, Etoh T, Muramatsu T, Kawamura K, et al. Lack of evidence for reovirus infection in tissues from patients with biliary atresia and congenital dilatation of the bile duct. J Hepatol. 2004; 40:203–211. [PubMed: 14739089]
36. Bessho K, Mourya R, Shivakumar P, Walters S, Magee JC, Rao M, Jegga AG, et al. Gene expression signature for biliary atresia and a role for interleukin-8 in pathogenesis of experimental disease. Hepatology. 2014; 60:211–223. [PubMed: 24493287]
37. Li J, Bessho K, Shivakumar P, Mourya R, Mohanty SK, Dos Santos JL, Miura IK, et al. Th2 signals induce epithelial injury in mice and are compatible with the biliary atresia phenotype. J Clin Invest. 2011; 121:4244–4256. [PubMed: 22005305]
38. Stipanuk MH, Dominy JE Jr. Lee JI, Coloso RM. Mammalian cysteine metabolism: new insights into regulation of cysteine metabolism. J Nutr. 2006; 136:1652S–1659S. [PubMed: 16702335]
39. Dahl EL, Mulcahy RT. Cell-type specific differences in glutamate cysteine ligase transcriptional regulation demonstrate independent subunit control. Toxicol Sci. 2001; 61:265–272. [PubMed: 11353135]
40. Strazzabosco M, Fabris L. Development of the bile ducts: essentials for the clinical hepatologist. J Hepatol. 2012; 56:1159–1170. [PubMed: 22245898]
41. Parola M, Cheeseman KH, Biocca ME, Dianzani MU, Slater TF. Biochemical studies on bile duct epithelial cells isolated from rat liver. J Hepatol. 1990; 10:341–345. [PubMed: 1973179]
42. Chanas SA, Jiang Q, McMahon M, McWalter GK, McLellan LI, Elcombe CR, Henderson CJ, et al. Loss of the Nrf2 transcription factor causes a marked reduction in constitutive and inducible expression of the glutathione S-transferase Gsta1, Gsta2, Gstm1, Gstm2, Gstm3 and Gstm4 genes in the livers of male and female mice. Biochem J. 2002; 365:405–416. [PubMed: 11991805]
43. Celli A, Que FG, Gores GJ, LaRusso NF. Glutathione depletion is associated with decreased Bcl-2 expression and increased apoptosis in cholangiocytes. Am J Physiol. 1998; 275:G749–757. [PubMed: 9756506]

44. Kwan KM, Fujimoto E, Grabher C, Mangum BD, Hardy ME, Campbell DS, Parant JM, et al. The Tol2kit: a multisite gateway-based construction kit for Tol2 transposon transgenesis constructs. Dev Dyn. 2007; 236:3088–3099. [PubMed: 17937395]

45. Wilkins BJ, Lorent K, Matthews RP, Pack M. p53-mediated biliary defects caused by knockdown of cirh1a, the zebrafish homolog of the gene responsible for North American Indian Childhood Cirrhosis. PLoS One. 2013; 8:e77670. [PubMed: 24147052]

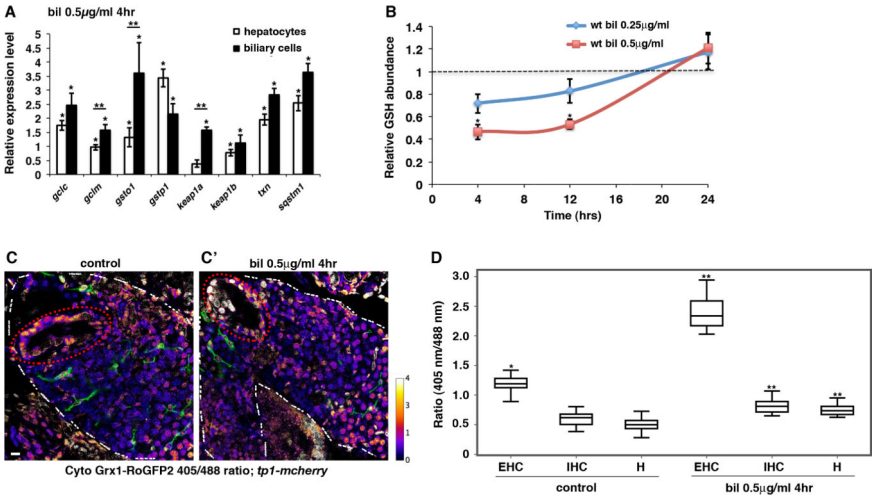

Fig. 1. Biliatresone induces redox stress and activates the Keap1-Nrf2 signaling pathway

(A) Graphical representation of Nrf2 target gene expression in biliatresone-treated (0.50 μg/ml, 4 hr) larvae *versus* DMSO-treated controls as determined by nCounter technology. Combined biliary cell (EHC & IHC) and hepatocyte polysome mRNA was isolated by the translating ribosomal affinity purification (TRAP) methodology. Data represent mean of three experiments with 50-100 larvae dissected per condition for each experiment. Error bars, standard error of the mean (41). *$p < 0.03$ in comparison to DMSO-treated controls, **$p < 0.05$, hepatocytes versus biliary cells. (B) Hepatic GSH levels after 4 hr, 12 hr and 24 hr of treatment with biliatresone compared with sibling control larvae by mass spectrometry. GSH level set as 1 for DMSO-treated controls (dashed line). Data show mean values for three experiments with five larvae per group per experiment. Error bars, SEM. *$p < 0.005$ in comparison to controls. (C-C') *In situ* measurement of GSH redox status. Representative composite confocal projections through the livers of control (C) and biliatresone-treated (0.50 μg/ml, 4 hr) (C') *Tg(ef1:Grx-roGFP2; Tp1:mCherry)* larvae scanned at 405 nm and 488 nm excitation wavelengths. GSH redox status of EHC (gallbladder – dashed red circle), IHC, and hepatocytes derived from the ratio of fluorescence emission (405nm/488nm). Color bar on right (higher ratio number indicates more oxidation). EHC and hepatocytes localized by morphology. IHC localized by mCherry expression (pseudo-colored green to show location relative to hepatocytes). White dashed line – liver border. Scale bar, 20 μm. (D) Median fluorescent emission ratios at 405 nm and 488 nm excitation wavelengths in EHC, IHC and hepatocytes. n=10 larvae for each condition. Boxes bound 1st and 3rd quartiles; whisker, ±1.5 IQR. *$p < 0.001$ in comparison to control hepatocytes, **$p < 0.01$ in comparison to control EHC, IHC, or hepatocytes, respectively. Abbreviations: bil, biliatresone; EHC, extrahepatic cholangiocytes; H, hepatocytes; IHC, intrahepatic cholangiocytes; IQR; interquartile range; wt, wild-type.

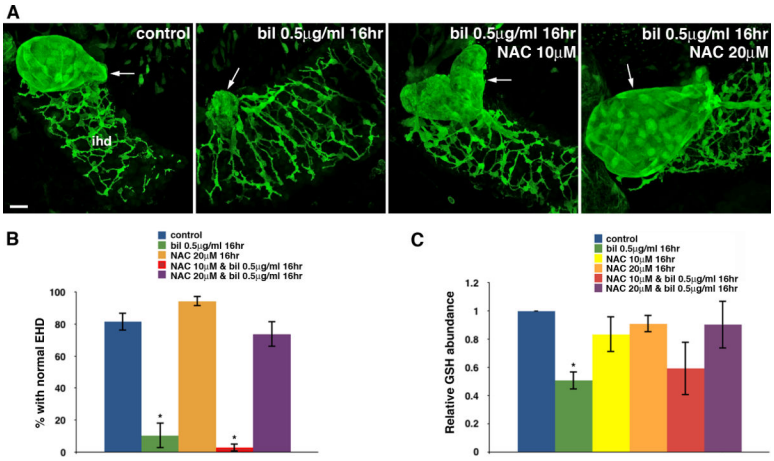

Fig. 2. *N*-acetylcysteine inhibits biliatresone toxicity

(A) Confocal projections through the livers of 6 dpf wild-type control and sibling larvae treated with either biliatresone (0.50 μg/ml), or biliatresone and NAC, for 16 hr. Larvae were immunostained with anti-Annexin A4 antibody. Treatment with biliatresone disrupts gallbladder morphology (arrow); however, this is prevented by NAC at 20 μM. The gallbladder remained deformed with abnormal contour after co-incubation with NAC at 10 μM. Scale bar, 20 μm. (B) Percentage of control larvae and siblings exposed to either biliatresone or biliatresone and NAC with normal EHD morphology. *$p < 0.001$ compared to control larvae. (C) Relative hepatic GSH levels of biliatresone–treated larvae with or without NAC co-treatment (*$p < 0.05$) compared to control larvae. All data represent mean of at least three experiments with 5-10 larvae per condition for each experiment. Error bars, SEM. Abbreviations: bil, biliatresone; EHD, extrahepatic bile duct; IHD, intrahepatic bile ducts; NAC, *N*-acetylcysteine.

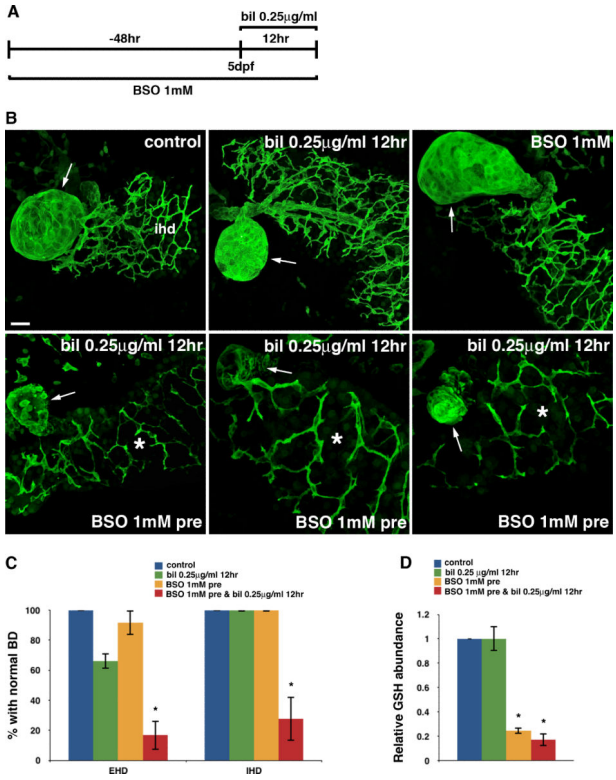

Fig. 3. GSH depletion sensitizes cholangiocytes to biliatresone

(A) Experimental scheme depicting treatment of 3 dpf wild-type larvae with BSO (1 mM) for 48 hr prior to low-dose biliatresone exposure at 5 dpf (0.25 μg/ml, 12 hr). (B) Confocal projections through the livers of 5 dpf larvae immunostained with anti-Annexin A4 antibody. The top three images show control, biliatresone-treated, and BSO-treated larvae. Morphology of the gallbladder (arrow) and IHD is normal in the control larva and larvae treated with low-dose biliatresone or BSO. In contrast, significant destruction of both the EHD (gallbladder-arrow) and IHD (*) is noted in biliatresone-treated larvae preconditioned with BSO (bottom panels). Scale bar, 20 μm. (C) Percentage of larvae exposed to biliatresone or biliatresone and BSO with normal EHD and IHD morphology. *$p < 0.001$ compared to control larvae. (D) Hepatic GSH levels in low-dose biliatresone-treated larvae with and without BSO pretreatment. *$p < 0.001$ compared to control larvae. All data represent mean of at least three experiments with 5-10 larvae per condition for each experiment. Error bars, SEM. Abbreviations: bil, biliatresone; BD, bile duct; BSO, buthionine sulfoximine; EHD, extrahepatic bile duct; IHD, intrahepatic bile ducts.

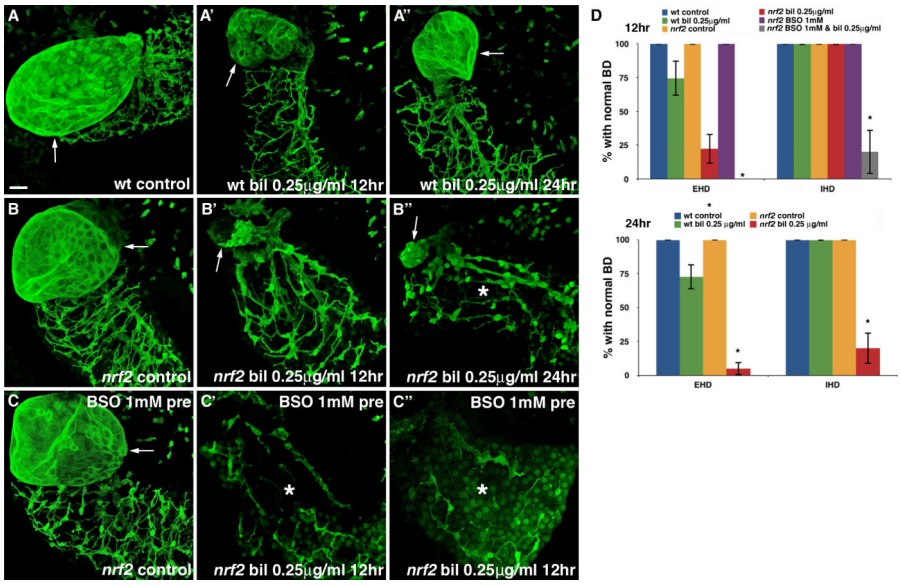

Fig. 4. Nrf2 inactivation sensitizes cholangiocytes to biliatresone

(A-A") Confocal projections through the livers of a 6 dpf immunostained (anti-Annexin A4 antibody) wild-type (wt) control larva (A) and sibling larvae treated with low-dose biliatresone (0.25 μg/ml) for 12 hr (A') and 24 hr (A"). The gallbladder (arrow) and IHD morphology remain normal after low-dose biliatresone incubation. (B-B") Confocal projections through the livers of an identically processed *nrf2*$^{fh318/f3h318}$ (*nrf2*) control larva (B) and sibling *nrf2* mutants treated with low-dose biliatresone for 12 hr (B') and 24 hr (B"). Gallbladder (arrow) destruction is evident in the biliatresone-treated larva at 12 hr. At 24 hr, the IHD (*) appear hypoplastic. (C-C") Confocal projections through the livers of identically processed *nrf2* mutants pre-conditioned with BSO. Severe gallbladder and IHD (*) injury is evident in larvae treated with BSO and biliatresone. Scale bar, 20 μm. (D) Percentage of wt and *nrf2* mutants exposed to low-dose biliatresone, BSO, or a combination of both, with normal EHD and IHD morphology. Data represent mean of at least three experiments with 5-10 larvae per condition for each experiment. Error bars, SEM. *$p < 0.001$ compared to wt control larvae. Abbreviations: bil, biliatresone; BD, bile duct; BSO, buthionine sulfoximine, EHD, extrahepatic bile duct; IHD, intrahepatic bile ducts; *nrf2*, *nrf2*$^{fh318/fh318}$, wt, wild-type.

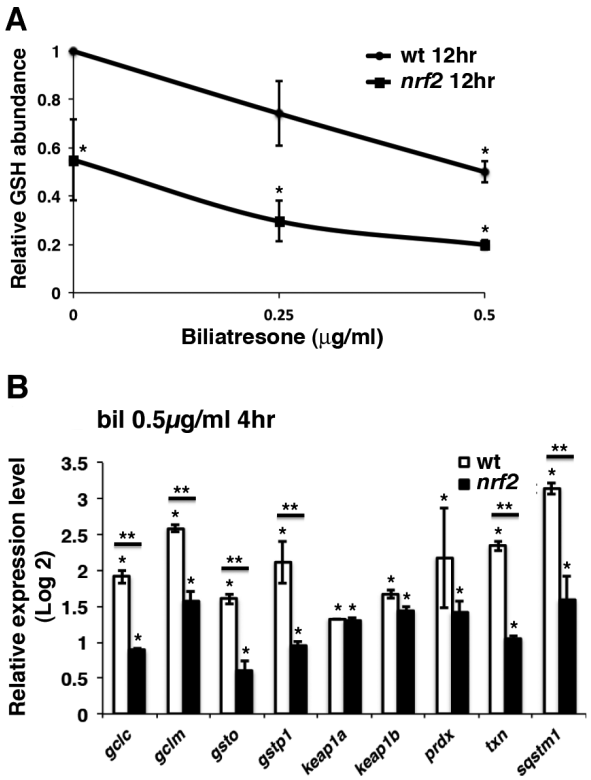

Fig. 5. Nrf2 inactivation reduces hepatic GSH reserve

(A) Hepatic GSH levels in wild-type (wt) and sibling *nrf2*$^{fh318/fh318}$ (*nrf2*) larvae normalized to wt controls. Data represent mean of three experiments with five larvae per condition for each experiment. Error bars, SEM. *p < 0.03 compared to wt control larvae. (B) nCounter analysis of Nrf2 target gene expression in livers of wt and *nrf2* mutant larvae with and without biliatresone treatment. Data represent mean of three experiments with 30 larvae dissected per condition for each experiment. Error bars, SEM. *p < 0.03 in comparison to DMSO-treated controls, **p < 0.03, wt versus *nrf2* mutants. Abbreviations: *nrf2*, *nrf2*$^{fh318/fh318}$; wt, wild-type.

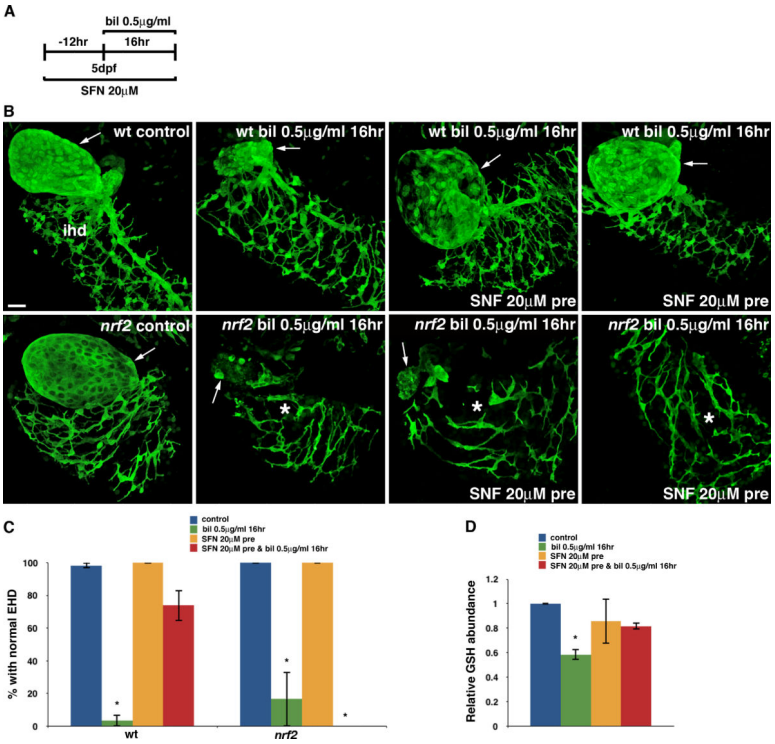

Fig. 6. Nrf2 activation inhibits biliatresone toxicity

(A) Experimental scheme depicting pre-treatment of larvae with sulforaphane (SFN), a known Nrf2 activator, followed by incubation with biliatresone (0.5 μg/ml, 16 hr). (B) Top panels show confocal projections through the livers of a 6 dpf immunostained (anti-Annexin A4 antibody) wild-type (wt) control and sibling larvae treated with biliatresone or biliatresone and SFN. Gallbladder (arrow) injury is inhibited with SFN pretreatment. Lower panels show representative images of identically processed *nrf2*$^{fh318/fh318}$ (*nrf2*) larvae. In contrast to the wt larvae, SFN does not inhibit biliatresone toxicity in *nrf2* mutants. Scale bar, 20 μm. (C) Percentage of wt and *nrf2* larvae exposed to biliatresone or biliatresone and SFN with normal EHD morphology. *p < 0.005 compared to control larvae. (D) Relative hepatic GSH levels of biliatresone–treated wt larvae with or without SFN pre-treatment. *p < 0.001 compared to control larvae. All data represent mean of at least three experiments with 5-10 larvae per condition for each experiment. Error bars, SEM. Abbreviations: bil, biliatresone; EHD, extrahepatic bile duct; IHD (*), intrahepatic bile ducts; *nrf2*, *nrf2*$^{fh318/fh318}$; SFN, sulforaphane; wt, wild-type.